Perpendicular magnetic anisotropy in ultrathin *Co|Ni* multilayer films studied with ferromagnetic resonance and magnetic x-ray microspectroscopy

F. Macià[a], P. Warnicke[b], D. Bedau[a], M.-Y. Im[c], P. Fischer[c], D.A. Arena[b], A.D. Kent[a]

[a] Department of Physics, New York University, 4 Washington Place, New York, NY 10003, USA

[b] National Synchrotron Light Source, Brookhaven National Laboratory, Upton, NY 11973, USA

[c] Center for X-ray Optics, Lawrence Berkeley National Laboratory, Berkeley, CA 94720, USA

Abstract

Ferromagnetic resonance (FMR) spectroscopy, x-ray magnetic circular dichroism (XMCD) spectroscopy and magnetic transmission soft x-ray microscopy (MTXM) experiments have been performed to gain insight into the magnetic anisotropy and domain structure of ultrathin *Co|Ni* multilayer films with a thin permalloy layer underneath. MTXM images with a spatial resolution better than 25 nm were obtained at the Co L_3 edge down to an equivalent thickness of Co of only 1 nm, which establishes a new lower boundary on the sensitivity limit of MTXM. Domain sizes are shown to be strong functions of the anisotropy and thickness of the film.

Highlights

► We show record sensitivity of x-ray microscopy in a 1 nm Co effective thickness. ► We found extreme sensitivity of the domain structure to number of bilayer repeats. ► Perpendicular anisotropy is nearly independent of the number of bilayers. ► We have combined Ferromagnetic resonance and high resolution XMCD microscopy.

Keywords

- Perpendicular magnetic anisotropy;
- Domain imaging;
- Ferromagnetic resonance (FMR);
- X-ray microscopy;
- X-ray magnetic circular dichorism

Ultrathin ferromagnetic films with perpendicular anisotropy are of interest for novel spin-based devices, such as spin-transfer torque magnetic random access memories and spin-torque nano-oscillators [1] and [2]. In many cases, layer stacks that consist of magnetic layers with different easy axis directions can improve spin-transfer device performance and are therefore the focus of current device physics studies [3] and [4]. Practical devices need low current for magnetization switching as well as stability against thermal noise; devices with perpendicular magnetic anisotropy combine both. Multilayers of *Co|Ni* have perpendicular magnetic anisotropy and high spin polarization and are thus suitable for spin current devices.

State-of-the-art characterization methods are needed to determine the properties of individual magnetic layers in the composite layer stacks to directly resolve magnetic behavior of each individual layer. This is essential to understand the interplay between magnetic interactions (e.g., exchange, magnetostatic, and magnetic anisotropy) in determining the layers magnetic response and domain structure. Magnetic domain structures and magnetic-moment dynamics are complex and rich in ferromagnetic thin films—and so are they in devices using ferromagnetic thin films. Magnetic domain structures and vortices may effect the efficiency of devices. Imaging techniques are thus essential to complement the broad set of electronic transport techniques used in studying nanomagnetic devices.

The inherent element-specificity of x-ray magnetic circular dichroism (XMCD) based spectroscopies and microscopies provides a unique and direct means to monitor the magnetic behavior of individual layers within a complex and multicomponent stack of layers. In this letter we demonstrate that XMCD microspectroscopy in combination with ferromagnetic resonance (FMR) spectroscopy allows us to gain insight into subtle changes of the magnetic properties and magnetic domain structure of an ultrathin magnetic layer with perpendicular magnetic anisotropy in a composite system.

We have deposited *Co*|*Ni* multilayers, capped with Pt, on a permalloy (Py), Cu base layer by evaporation in an ultra high vacuum chamber. The samples, with a complete layer stack |3 *Ta*|50 *Cu*|3 *Ta*|10 *Py*|10 *Cu*|[0.2 *Co*|0.6 *Ni*]×*n*|0.2 *Co*|5 *Pt*| (thicknesses in nanometers), were deposited on silicon nitride (Si_3N_4) membranes supported by Si substrate frames to allow for x-ray transmission. The thickness of the Cu spacer layer, 10 nm, was chosen to magnetically decouple the in-plane magnetized Py layer from the out-of-plane magnetized *Co*|*Ni* multilayer. A *Co*|*Pt* capping layer was used to further enhance the interface-induced perpendicular magnetic anisotropy of the *Co*|*Ni* multilayer [7]. To address the influence of the number of bilayers, three different samples with n=4, 6, and 8, repeats were studied.

In order to determine the magnetic anisotropy of the films we conducted FMR spectroscopy with frequencies ranging from 4 to 40 GHz as a function of the applied field at room temperature. To record the weak signals of the ultrathin magnetic layers we used a coplanar waveguide (CPW) with a smooth signal transmission within this frequency range. The absorption signal was recorded by sweeping the magnetic field at constant frequency with the sample mounted ‘flip-chip’ on the CPW [5] and [6]. Fig. 1 shows the frequency dependence (f) of the resonant field (H_r) for a configuration of an applied field perpendicular to the film plane, as shown in the inset of Fig. 1. The resonant condition is given by [5]

$$f = \frac{\gamma}{2\pi}\left(\mu_0 H_r - \mu_0 M_s + \frac{2K}{M_s}\right),$$

where γ is the gyromagnetic ratio, M_s is the saturation magnetization and K is the perpendicular magnetic anisotropy constant. The f=0 intercept of the resonance curve enables a determination of the magnetic anisotropy (i.e., $\mu_0 M_s - (2K/M_s)$) and the slope of the resonance curve gives the gyromagnetic ratio.

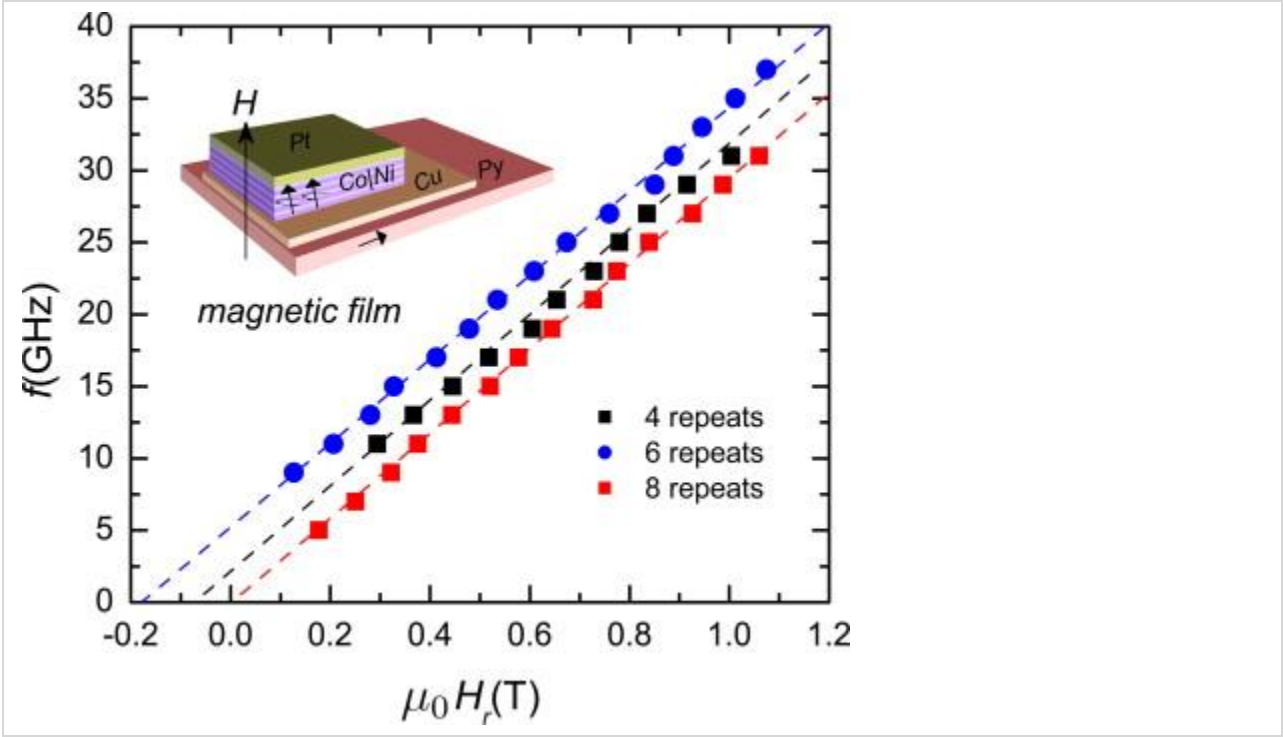

Fig. 1. FMR results: frequency dependence of the resonant field versus applied field perpendicular to the film plane. The dashed lines are fits using Eq. (1). The inset shows a schematic of the sample layer stack and the magnetic moments orientations of *Co|Ni* and Py layers.

We have estimated M_s from nominal bulk magnetizations of Ni and Co accounting for the extra Co layer: M_s≃7.57×10^5, M_s≃7.45×10^5 and $M_s \simeq 7.38 \times 10^5$ A/m for 4, 6, and 8 repeats, respectively. Perpendicular anisotropies of the three films slightly differ: $K \simeq 3.89 \pm 0.05 \times 10^5$ J/m^3, $4.14 \pm 0.03 \times 10^5$ J/m^3, and $3.42 \pm 0.02 \times 10^5$ J/m^3 for 4, 6, and 8 repeats, respectively. The gyromagnetic ratio γ is $\simeq 1.84 \pm 0.035 \times 10^{11}$ Hz/T (i.e., g≃2.09±0.04) for the three samples (which is a bit lower than those found for *Co|Ni* in [5]). The anisotropy of a multilayered structure remains nearly constant with the number of bilayer repeats (if the repetition unit is constant). Our multilayer structures have two extra interfaces–Co and Pt–that break the repetition unit of *Co|Ni* because they do not scale with the number of repeats. Previous research has established that there is a perpendicular magnetic anisotropy associated with *Co|Pt* interfaces for ultrathin Co thicknesses (< 1.4 nm) [7]. The extra *Co|Pt* interface enhances perpendicular magnetic anisotropy and their relative importance is expected to decrease with increasing number of *Co|Ni* bilayer repeats. Thus, the anisotropy is expected to decrease somewhat with the number of bilayer repeats. Variations of 5–10% of nominal thicknesses–and thus, of their anisotropies – may arise from fabrication conditions in such ultrathin multilayers.

Samples with n=4 and n=6 have perpendicular anisotropy that overcomes the shape anisotropy of the film ($\mu_0 M_s < 2K/M_s$); the other one, n=8, does not (in this case $\mu_0 M_s = 2K/M_s$). However, the thin film with n=8 still has a preferred out-of-plane axis because magnetic moments form stripe domains that reduce the

magnetostatic energy of the out-of-plane configuration (i.e., magnetization of the sample n=8 will only be isotropic if we consider it to behave as a single magnetic domain). Note that for large fields (approx 1 T) the Py magnetization will rotate out of the film plane and may effect the FMR measurement of the *Co*|*Ni* multilayer. However, no or very few domains are present in such a magnetization process so the magnetization in the Py is uniform and the resulting fringe fields in the *Co*|*Ni* multilayer will be very small. We have performed in-plane field ferromagnetic resonance measurements to observe the Py behavior and we have found there is no observable change in the Py resonance frequency that we can associate with interlayer coupling.

To understand better the microscopic origin of the perpendicular magnetic anisotropy in these systems, XMCD spectroscopy and element-specific hysteresis loops were measured at beam line U4B at the National Synchrotron Light Source (NSLS). X-ray absorption spectroscopy (XAS) and XMCD spectra taken across the Co L_3 and L_2 edges (see Fig. 2(a)) indicate clean, unoxidized Co layers; similar results were obtained for the Fe and Ni edges (not shown). Element-specific hysteresis loops shown in Fig. 2(b) and (c) were measured by tuning the photon energy to the L_3 edges of Co, Ni, and Fe and sweeping the out-of-plane magnetic field from an initial value of +700 mT (substantially larger than the saturation field of $\sim 100\ \mathrm{mT}$). The loops for Co and Fe isolate the magnetic contributions from the *Co*|*Ni* and Py layers, respectively, while loops for the Ni (not shown) display a composite picture with contributions from both the Py and *Co*|*Ni* layers. As expected, the Fe hysteresis loops shows a hard axis behavior consistent with the in-plane anisotropy of the Py layer. The Co hysteresis loops show that the n=4 and $n = 6\ \mathrm{Co|Ni}$ films have a large remanence and coercive fields ($\mu_0 H_c$) of 40 mT (n=4) and 85 mT (n=6). The n=8 film, on the other hand, has a smaller $\mu_0 H_c$ of 25 mT as well as a lower susceptibility around H_c. The Co hysteresis loops and H_c correlate well with K determined from our FMR measurements (see Table 1).

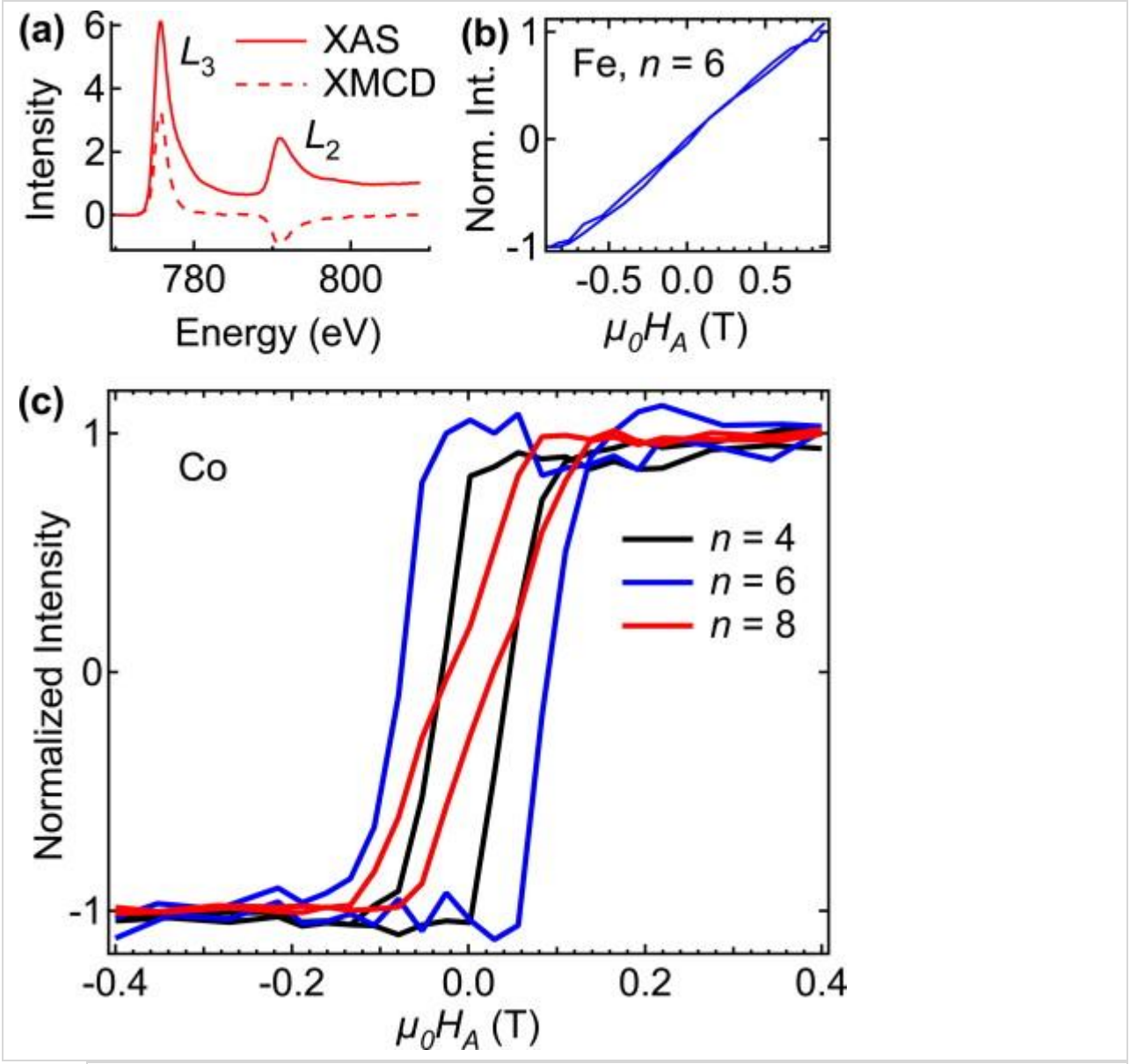

Fig. 2. (a) Energy scans of the XAS and XMCD spectra for n=8. (b) Element specific hysteresis measurements for n=6 obtained at the Fe L_3 edge with an out-of-plane applied field, showing a hard axis magnetic response. (c) Element-specific hysteresis loops for different bilayer repeats obtained at the Co L_3 absorption edge using out-of-plane applied magnetic fields.

Table 1. Comparison of the anisotropies, K, coercive fields, H_c, and magnetic domain sizes D at the coercive field for different multilayer repeats. Data obtained from FMR, element specific hysteresis loops and XMCD images respectively.

n	K (J/m^3)	$\mu_0 H_c$ (mT)	D(H_c) (nm)
4	3.89±0.03×10^5	40±4	210
6	4.14±0.05×10^5	85±6	280
8	3.42±0.02×10^5	25±2	100

These results were correlated with the microscopic magnetic domain structure by performing magnetic transmission soft x-ray microscopy measurements at beamline 6.1.2 (XM-1) at the Advanced Light Source in Berkeley. X-ray images with a spatial resolution of better than 25 nm were obtained at the Co L_3 absorption edge [8]. To reduce non-magnetic background and to account for non-uniform illumination the x-ray images have been normalized to a magnetically flat image (i.e., images show differences from an initial image taken at the beginning of each magnetic loop under a large negative perpendicular magnetic field). Fig. 3 shows the evolution of the magnetic domain structures at various applied magnetic fields for the multilayered samples. It can be seen that the dominant magnetization reversal mechanism is governed by domain nucleation, growth, and annihilation. We note that the magnetic domain patterns observed over a microscopic field of view directly correlate with the element specific hysteresis loops derived from XMCD spectroscopy, which cover a macroscopic area of the sample of 0.5 mm in size. The measured contrast in images shown in Fig. 3 was 3–4%, 5–6% and 7–8% for n=4, 6 and 8 respectively. It is worth noting that the clear observation of the magnetic domain pattern down to an effective Co thickness of 1 nm demonstrates a high sensitivity of the XMCD contrast in full field soft x-ray microscopy.

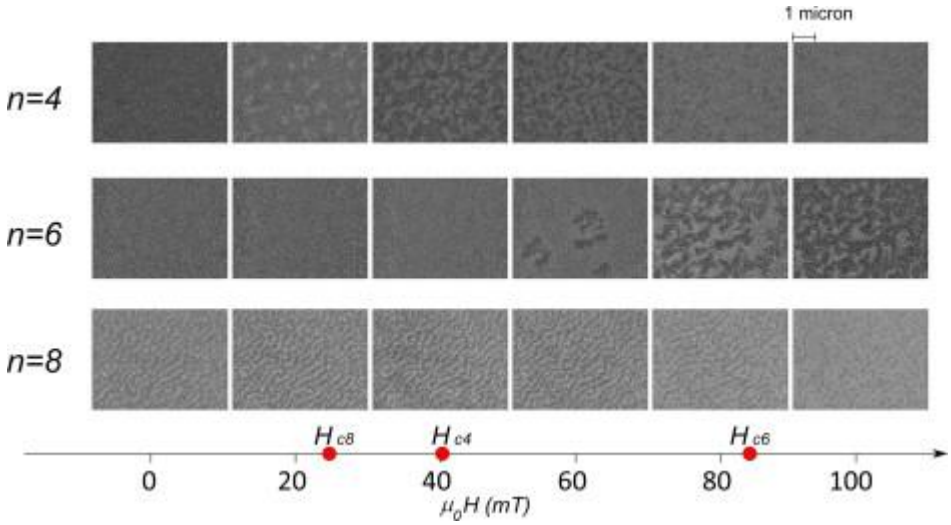

Fig. 3. Evolution of the magnetic domain structure in samples with different number of bilayer repeats as a function of the external applied magnetic field. The MTXM images were recorded at the Co L_3 edge with the field applied perpendicular to the film plane. The dots indicate the coercive fields determined from XMCD hysteresis loops (cf. Fig. 2).

We determined an averaged value for the domain sizes (listed in Table 1) by repeatedly measuring the domain width across domains (10–90% change in intensity of the filtered images) along different directions. We found that the characteristic domain size is significantly smaller in the film with the largest number of bilayer repeats, n=8. This is associated with the competition between magnetic interactions. Specifically, the dipolar or magnetostatic interactions favor subdivision of the film into small-scale domains while the exchange and anisotropy interactions favor uniformly magnetized states [9], [10] and [11]. Qualitatively, in a film with perpendicular anisotropy, increasing the film thickness increases

the importance of the magnetostatic energy relative to the exchange and anisotropy energies and leads to reduced domain size; conversely, increasing the magnetic anisotropy decreases the importance of the magnetostatic energy and leads to larger domain size. More quantitatively, there is a characteristic length scale that depends on the ratio of the domain wall to the magnetostatic energies: $D_0 = 8\sqrt{AK}/(\mu_0 M_s^2)$, where A is the exchange constant [12]. Films with thickness less than D_0 are in a limit in which the zero-field equilibrium domain size decreases rapidly ($D(H=0) \sim t\exp(\pi D_0/2t)$) with increasing film thickness t. Taking $A \approx 10^{-11}$ J/m we estimate $D_0 \simeq 22$ nm, putting our films in this ultrathin limit. Thus the appearance of small-scale domains near zero field (Fig. 3, n=8 with t=6.4 nm) correlates well with the film's increased thickness and reduced anisotropy. The other films n=4 and 6 have a high remanence and submicron scale domain subdivision is not observed in zero field.

To summarize, this study highlights the power of combining macroscopic and microscopic analytical techniques to understand the magnetic properties of ultrathin magnetic films. FMR provided a quantitative measurement of the anisotropy fields, whereas element specific hysteresis loops determined the coercive fields and the evolution of macroscopic magnetization. A link to the microscopic origin was obtained with high resolution XMCD microscopy allowing observation of the evolution of the domain structure as a function of the applied field and a measurement of the change in characteristic domain widths. We have shown sensitivity of x-ray microscopy for layers down to 1 nm effective thickness, which establishes a new lower boundary on the sensitivity limit of MTXM.

Acknowledgments

F.M. thanks support from Marie Curie IOF 253214 and from a Beatriu de Piniós from Catalan Government. Supported in part by ARO-MURI, Grant no. W911NF-08-1-0317. The operation of the microscope is supported by the Director, Office of Science, Office of Basic Energy Sciences, Materials Sciences and Engineering Division, of the U.S. Department of Energy under Contract no. DE-AC02-05-CH11231. Device fabrication was partly carried out at the Cornell Nanofabrication Facility.

References

[1] J. Katine, E.E. Fullerton
Journal of Magnetism and Magnetic Materials, 320 (2008), p. 1217

[2] F. Macià, A.D. Kent, F. Hoppensteadt
Nanotechnology, 22 (2011), p. 095301

[3] A.D. Kent, B. Ozyilmaz, E. del Barco
Applied Physics Letters, 84 (2004), p. 3897

[4] S. Mangin, D. Ravelosona, J.A. Katine, M.J. Carey, B.D. Terris, E.E. Fullerton
Nature Materials, 5 (2006), p. 210

[5] J.-M.L. Beaujour, W. Chen, K. Krycka, C.-C. Kao, J.Z. Sun, A.D. Kent
European Physical Journal B, 59 (2007), p. 475

[6] S. Girold, M. Gottwald, S. Andrieu, S. Mangin, J. McCord, E.E. Fullerton, J.-M.L. Beaujour, B.J. Krishnatreya, A.D. Kent

Applied Physics Letters, 94 (2009), p. 2009

[7] P.F. Carcia

Journal of Applied Physics, 63 (1988), p. 5066

[8] P. Fischer, D. Kim, W. Chao, J. Liddle, E. Anderson, D. Attwood

Materials Today, 9 (2006), p. 26

[9] C. Kittel

Physical Review, 70 (1946), p. 965

O. Hellwig, A. Berger, J.B. Kortright, E.E. Fullerton

Journal of Magnetism and Magnetic Materials, 319 (2007), p. 13

[11] R. Sbiaa, Z. Bilin, M. Ranjbar, H.K. Tan, S.J. Wong, S.N. Piramanayagam, T.C. Chong

Journal of Applied Physics, 107 (2010), p. 103901

[12] B. Kaplan, G.A. Gehring

Journal of Magnetism and Magnetic Materials, 128 (1993), p. 111

DISCLAIMER

This work was supported by the Director, Office of Science, of the U.S. Department of Energy under Contract No. DE-AC02-05CH11231.